

# Two-area power system stability analysis by frequency controller with UPFC synchronization and energy storage systems

Hossein Oghab Neshin<sup>1</sup>, \*Manouchehr Jandaghi Semnani<sup>2</sup>

<sup>1</sup>MSc of power engineering, Department of Mechatronic Engineering, Karaj Branch, Islamic Azad University, Alborz, Iran

<sup>2</sup>PhD, Assistant Professor, Department of Mechatronic Engineering, Karaj Branch, Islamic Azad University, Alborz, Iran

## Abstract:

*In recent years, the speed of the growth of electronic devices and switches has been remarkable and widely used for stability and control mechanisms in power system. If the disturbance persists for a long time then the conventional controllers for the LFC alone will not be enough to reduce the inconsistency between demand and production and results in frequency deviation from the nominal value. The proposed solution to overcome this problem is to use a frequency controller in coordination with Facts devices and energy storage systems. System control in emergency conditions and sudden changes of load will be studied and transient stability and system protection will be investigated. The control loop regulates the frequency and the actual power and the load-frequency voltage regulator loop controls the reactive power and voltage size. Accordingly, the frequency controller design is presented to improve the stability and prevent frequency deviations and disturbances in the power system. In this research, the small signal stability of a power network in which the load-frequency controller is in operation with facts and energy storage device is examined. Based on this, a new method using PSO algorithm is presented for optimization of the PID regulator used in a two-area power system as part of a load-frequency controller in conjunction with a UPFC and energy saving system. The efficiency of the proposed algorithm is proved in comparison with the classical algorithm of Nikles.*

**Keywords:** Frequency Control - Facts Devices - Bird Algorithm - PID Controller

## I. INTRODUCTION

The main purpose of controlling power systems is to produce the maximum electric power and maintaining an interconnected system in such a way that it is as reliable and economical as possible, while the voltages and frequencies are within the permitted limits [1, 2]. The power output of a generator is controlled by changing its input mechanical power. To do this, the steam flow or the water in the turbine

is adjusted to control the mechanical power and thus the active power output of the generator [3, 4]. If the power consumption of the load increases, a steam or a water valve should be opened to increase the generator's power output as much as possible, and if the power consumption of the load decreases, the valve should be closed to a certain extent and reduces the generating power of the generator and results in an active power balance. The power imbalance is felt by its effect on the speed or frequency of the generator. In case of reduction of load, the generator tends to increase its speed and frequency. For the case of load increase and lack of production, the speed and frequency of the generator are decreased. The frequency deviation from its nominal value is chosen as a signal to stimulate the automatic control system. The active power balance is an indicator of constant frequency of the system, and is of great importance. The corresponding control system is known as the Load-Frequency Control System (LFC). The LFC control loop only responds to modulation, slowness and frequency, and can't be controlled in an emergency and imbalance of power [5, 6]. System control in emergency and sudden changes is considered by studying transient stability and system protection. The change in actual power mainly affects the frequency of the system, while reactive power has little frequency sensitivity and is mainly dependent on voltage variations. Therefore, real and reactive power are controlled individually. The LFC frequency control loop controls real power and frequency and the voltage regulator loop regulates the reactive power and voltage size. With the increasing growth of interconnected power systems, frequency control has become more important and has enabled the operation of systems using new methods. It is now the basis of many advanced concepts for controlling large systems. In order a power system functions satisfactorily, a stable frequency is required. This is because the relatively precise control of the frequency causes stable operation of the synchronous and inductive motors, and motor speed stabilization is especially important in the satisfactory operation of production units, this

is due to the fact that these units heavily depend on the performance of all the peripheral stimuli associated with fuel, water, and combustion air supply systems [7, 8]. Also, in a network, a high frequency drop may causes severe magnetic fluxes in induction motors and transformers and finally causes irreparable damage. On the other hand, the widespread use of synchronous electric clocks and the use of frequency for other timekeeping purposes require the maintenance and precise timing of the synchronous time, which is proportional to the integral of frequency. So not only the frequency, but also its integral, should be regulated and controlled. In this research, the small signal stability of a power network in which the load-frequency controller (LFC) is in operation with facts and energy storage devices is examined. We use the PSO algorithm to select the optimal PID controller parameters for controlling the Load frequency of the two-area power system in presence of facts and storage devices.

**II. THE ORETICAL BASIS**

**Power System Stability:** The stability of a power system is, the ability of the power system to remain in equilibrium under normal operating conditions and to obtain a new balance point after a turbulence occurs. In general, in power system literature we encounter four types of static, dynamic, transient, and voltage stability [9].

The PSO is an optimization algorithm that operates on the basis of random population generation. The algorithm is based on the modeling and simulation of the collective flying of birds or collective movement of fishes. Each member of the group is defined by the vector of velocity and position in the search space. At each time interval, the new particle position is updated according to the current velocity vector and the best position found by that particle, and the best position found by the best particle in the group. The binary particle swarm optimization algorithm is presented in discrete mode with BPSO. In this algorithm, the position of each particle will be shown with a binary value of 0 or 1. In BPSO, the amount of each particle can change from 0 to 1 or from 1 to 0. The speed of each particle is also defined as the probability of changing the value of each particle to one [10]. The randomized generation of the initial population exists in almost all probabilistic optimization algorithms. But in this algorithm, in addition to the initial random location of particles, a value is also allocated for the initial particle velocity. The initial propagation range for particle velocity can be extracted from the following equation-1:

$$\frac{X_{min} - X_{max}}{2} \leq V \leq \frac{X_{max} - X_{min}}{2}$$

The Xmin and Xmax are the minimum and maximum values for the particle coordinates, respectively.

An increase in the number of particles causes the algorithm to spend more time in the particle evaluation stage, which increases the time of the evaluation so that the execution time of the algorithm, despite the decrease in the number of repetitions, does not decrease until the convergence is reached. So increasing the number of particles can't apply to reduce the algorithm runtime. In short, the number of primary population is determined by the problem. In general, the number of primary particles is a compromise between the parameters involved in the problem. Experimentally selecting a primary particle population of 20 to 30 particles is a good choice that can be applied to almost all test evaluations. We can consider the number of particles a bit more than what we normally need to have a little more safety margin when facing local minimums. The flowchart for the PSO algorithm is shown in Figure 1.

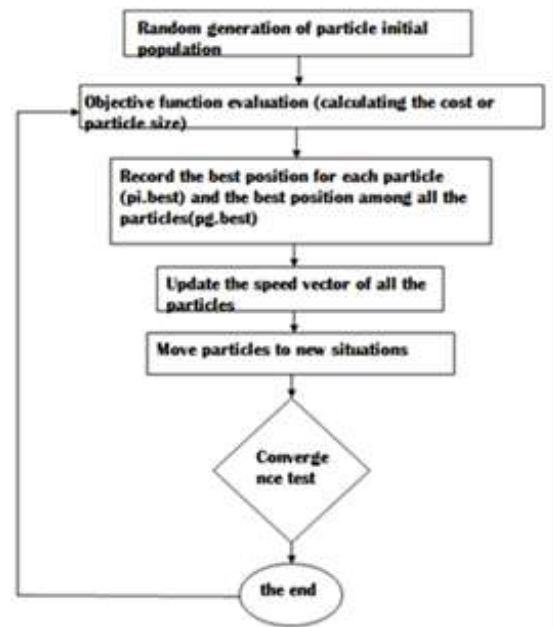


Figure1: Smart Search Particle Algorithm Flowchart [10]

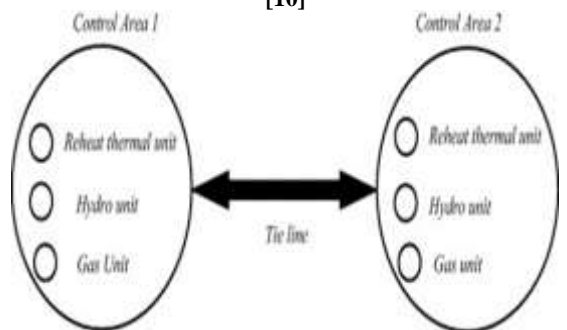


Figure 2 – Schematic view of a two-area system

**A. characteristics of two-area power network under study**

In this section, we consider a two-area system with three steam generators, a gas power plant with

combustion chamber and a water power plant with dropping slope of governor, which is connected to adjacent area through tie line, as shown in figure 2. All generators in the area are working simultaneously and are formed as a related group. Internal electrical connections in each area are very strong compared to connections with adjacent devices which are out of the region. In normal operation, each control area compensates the load changes in the area. Furthermore, every control area in a power system helps the establishment of frequency and voltage profile throughout the system. A multiregional system with internal connections, consists of several control regions that each of them absorbs the load changes in its area. Production share of each generator in every area is determined by the principles of the electric energy market. It is necessary for network frequency controller to have minimum settling time and the lowest oscillation, in order to control the frequency in unbalanced conditions of supply and demand. Besides, due to the defined capacity of each unit, it's necessary to have power compensator equipment such as UPFC and RFB power storage in the network, to compensate for any sudden changes in power consumption by area PID controllers, and to set frequency errors and line power deviations to zero by adjusting the frequency of each region and line power simultaneously. Proposed flowchart for the control system and Simulink model of two-area system are shown in figures 3 and 4, respectively.

Accordingly, participation factors for gas, water and steam power plants are 15%, 37% and 46%, respectively; dropping slope of governors are the same for all cases and equal to 2.4; UPFC time constant and power storage time constant are considered to be 0.01s and 0.78s, respectively. Detailed information of system parameters is available in [11].

**B. Optimization process with PSO optimization algorithm**

Now that power network modelling and frequency stability problem were explained in previous sections, in this section, problem statement needs to be formulated for optimization by PSO algorithm. Optimization steps are as follows:

- 1- Choose a few points of control coefficients (proportional, integral and derivative for

each area) according to [11], considering the design limits of controllers, and form the primary population of birds.

- 2- Calculate the fitness and cost of the objective function for each bird according to [11] and specify the dominant bird.

- 3- Set the route and flight speed of all birds in line with dominant bird.

- 4- Calculate the fitness and cost of the objective function for each bird searching for food [11] and specify the dominant bird.

- 5- If all the birds are at the same route and have constant speed, then stop calculations, otherwise we go back to step 3.

To solve this problem, we have used the capabilities of optimization toolbox in Matlab for 20 birds and 100 search iterations. The convergence plot of PSO algorithm to find minimum frequency error and line power is given in figure 5, in which sum of error squares is 0.81 and it is converged to minimum point at 20<sup>th</sup> iteration.

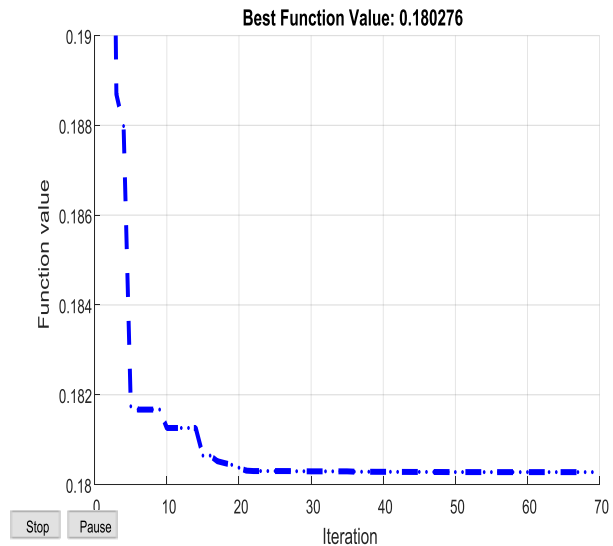


**Figure 5 – The convergence plot of PSO algorithm in search for optimum answer**

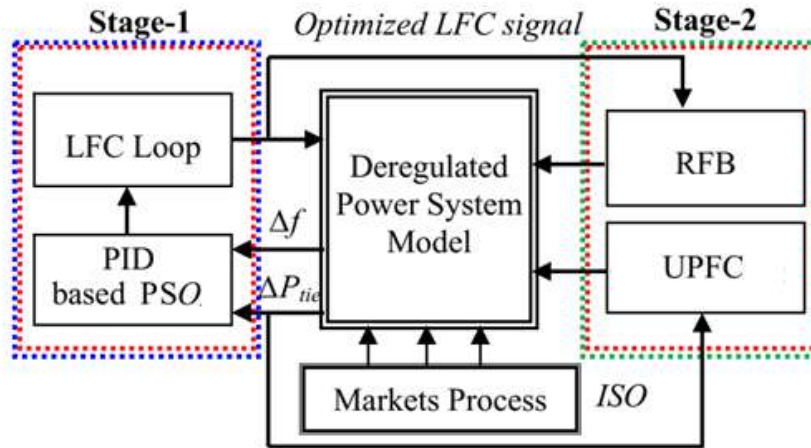


Figure 3 – proposed flowchart for the control system

I. TABLE 6 – OPTIMUM PARAMETERS FOR PROPOSED CONTROL SYSTEM

TWO AREA PID parameters	LFC area #1		LFC area #2	
	Ziegler-Nichols method	PSO Optimization	Ziegler-Nichols method	PSO Optimization
P	0.722	2.1	0.725	2.1
I	1.1959	2.1	1.082	2.1
D	-2.3044	1.04	-2.5586	0.691

ACE Performance Parameters	ACE area #1		ACE area #2	
	Ziegler-Nichols method	PSO Optimization	Ziegler-Nichols method	PSO Optimization
Rise Time (second)	3.78	3.69	4.05	3.15
Settle Time (second)	20.4	5.49	21.5	13.6
Overshoot (%)	2.99	2.49	2.97	2.43
Peak	1.03	1.02	1.03	1.02
Gain Margin (db)	14.4	4.47	14.2	9.82
Phase Margin (deg)	71.7	85.3	69	76.9

Optimization coefficients for controllers of these two areas using proposed method and Ziegler–Nichols classic method are given in Table 6, and in both areas the proportional and integral factors are constant and have been considered to be 2.1. As it is shown, settling time for step response of Area Control Error (ACE) to load changes in areas 1 and 2 are 5.49s and 31.6s, and their stability phase margins are 85.4 and 76.9 degrees, respectively, which indicate better stability in comparison with longer settling time and phase margins of Ziegler–Nichols method. The state equations of two-area power system with 2 input load

changes and 2 output frequency changes has 30 variables. The state variables and state matrix values are listed in [11].

### III. Research findings

#### A. Results of frequency control to changes in load in Area 1

changes in load, power generation is automatically adjusted so that the frequency is returned to the nominal value and the role of the PID controllers is

very influential. For this reason, we plan to examine the frequency fluctuations of the system in regions 1 and 2 and the oscillation of the power in the connection line for the changes of  $\Delta P_{L1} = 0/01pu$ . Simulation results are shown in Figure 7, which indicates the frequency control error in area 1 with the proposed method reaches to zero value in a shorter time and its settling time is less

than Ziegler–Nichols method. The control frequency error in the second region similar to the area 1 reaches to zero value in a shorter time and In both regions, the initial frequency error overshoots more than the classical method.

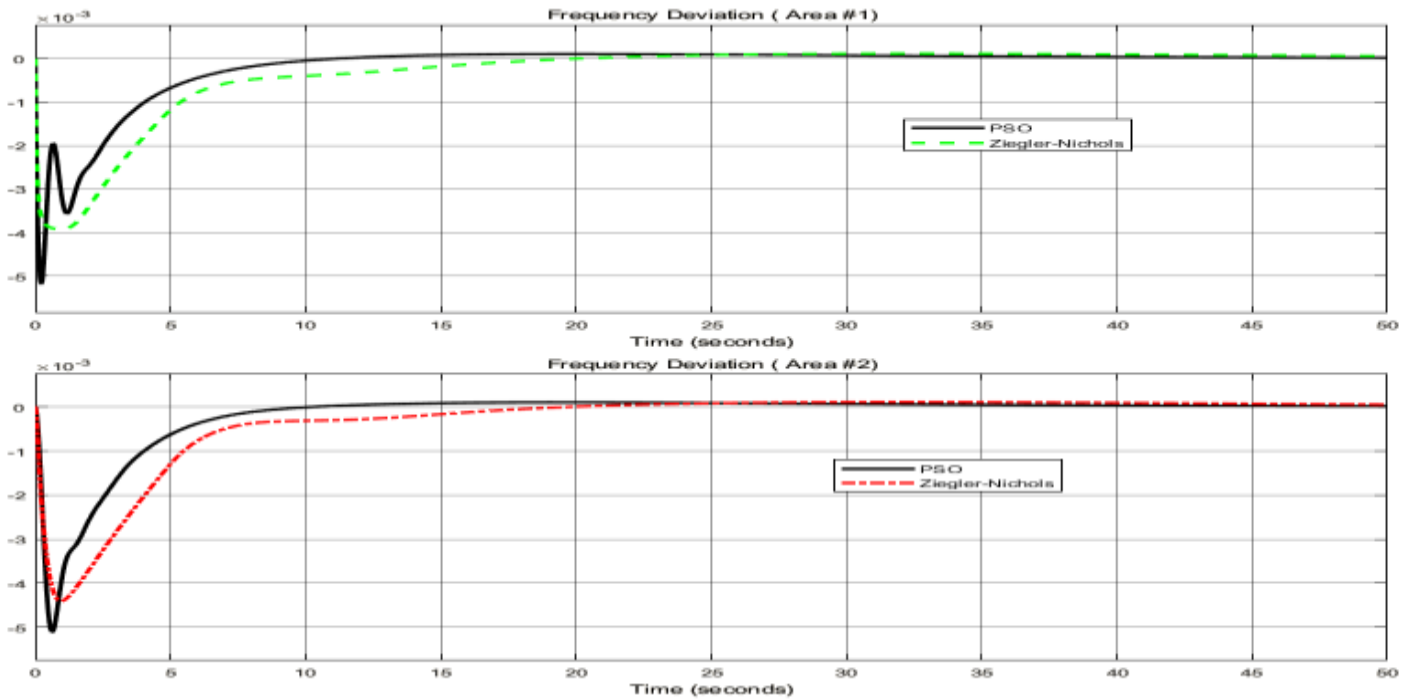


Figure7: Frequency deviation diagram to Load changes in area 1

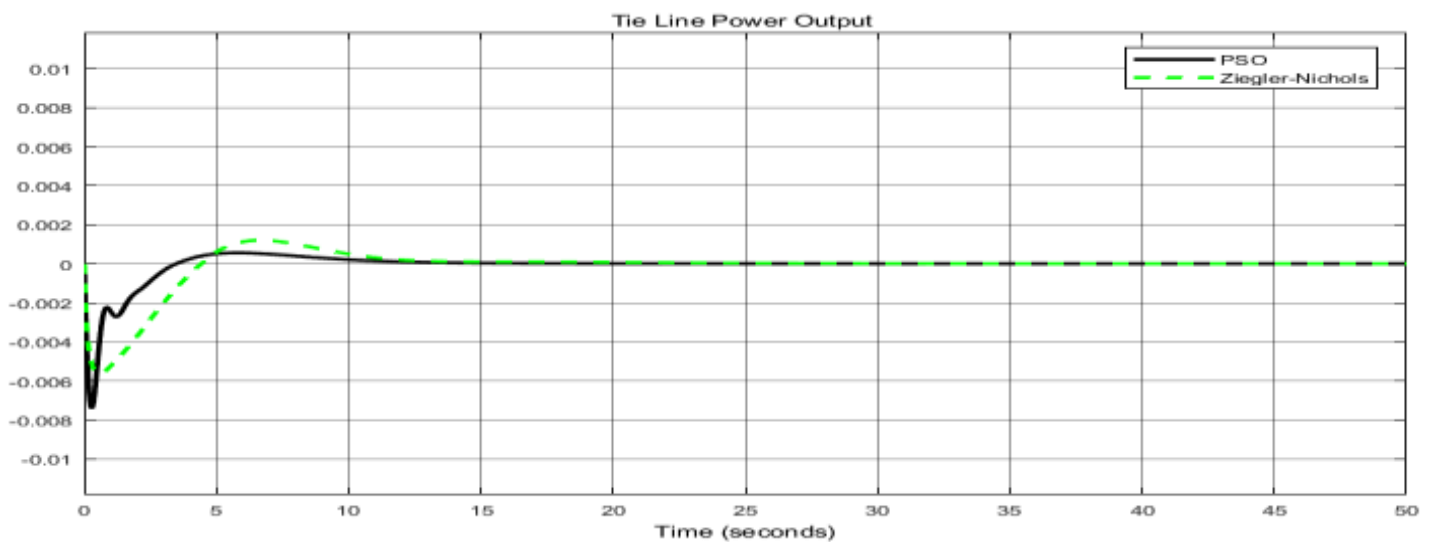


Figure8: Deviation of transmission line power to Load changes in area 1

Also, changes in the transmission line power between two regions, in terms of per unit, is shown in Figure 8, which indicates that the maximum oscillatory

power in tie line is equal to 0.006 per unit. This power fluctuates from the second region to the first region and its oscillations finally reaches to zero with

optimal performance of the controllers, and in the proposed method, the power oscillation is less than the classical method.

**B. Results of frequency control to changes in load in Area 2**

In this section, we intend to study the frequency oscillations of the system in regions 1 and 2 and the oscillation of the power in the connection line for  $\Delta P_{12} = 0/01pu$ . The simulation results are shown in Figure 9 which indicate the frequency control error in both regions, with classical and proposed methods encounter the maximum loss of frequency; and the

proposed controller has lower settling time. The magnitude of the integral of the square of frequency error for the proposed method and the classical method of Nichols for region one are 28.65 and 43.5 and for the second region, are 34.99 and 50.81 respectively, which indicate the efficiency of the proposed algorithm. To stabilize frequency due to

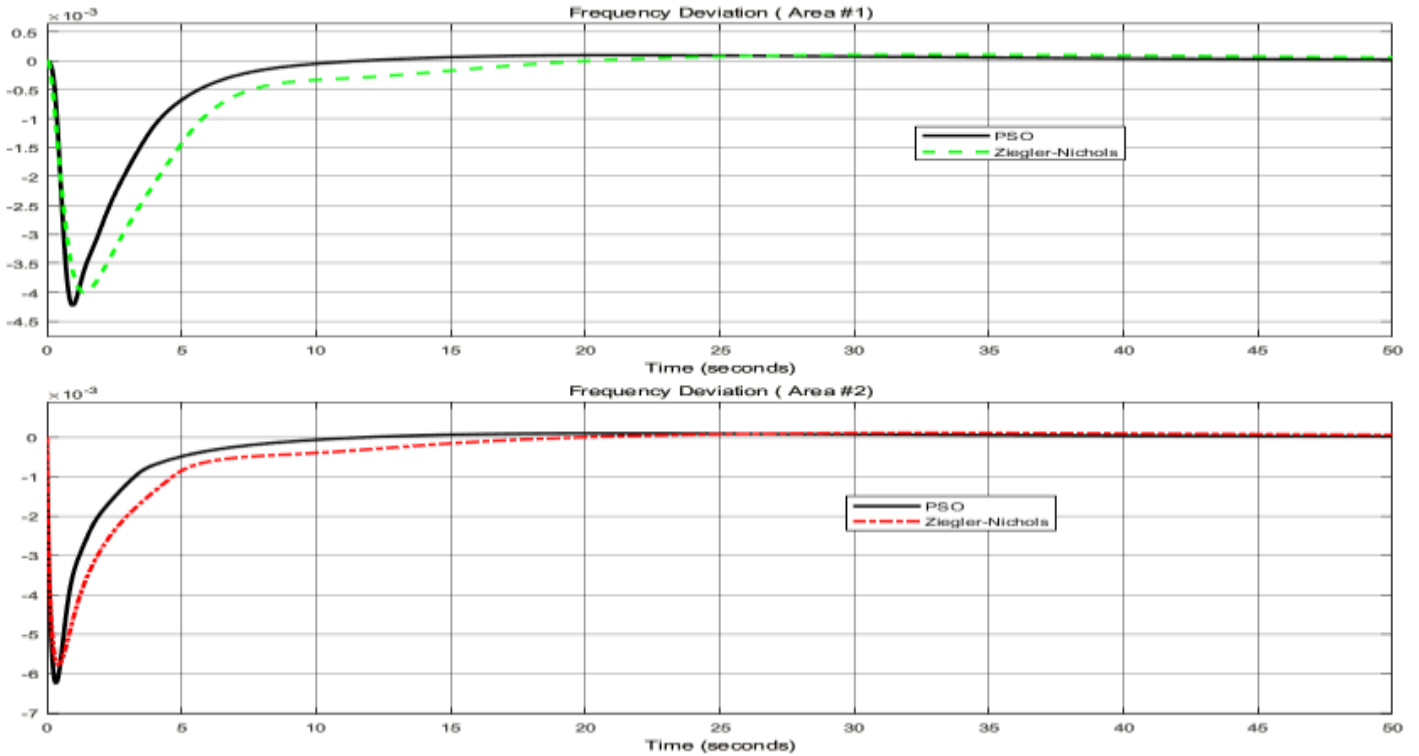


Figure 9: Frequency deviations of both regions to load changes in region 2

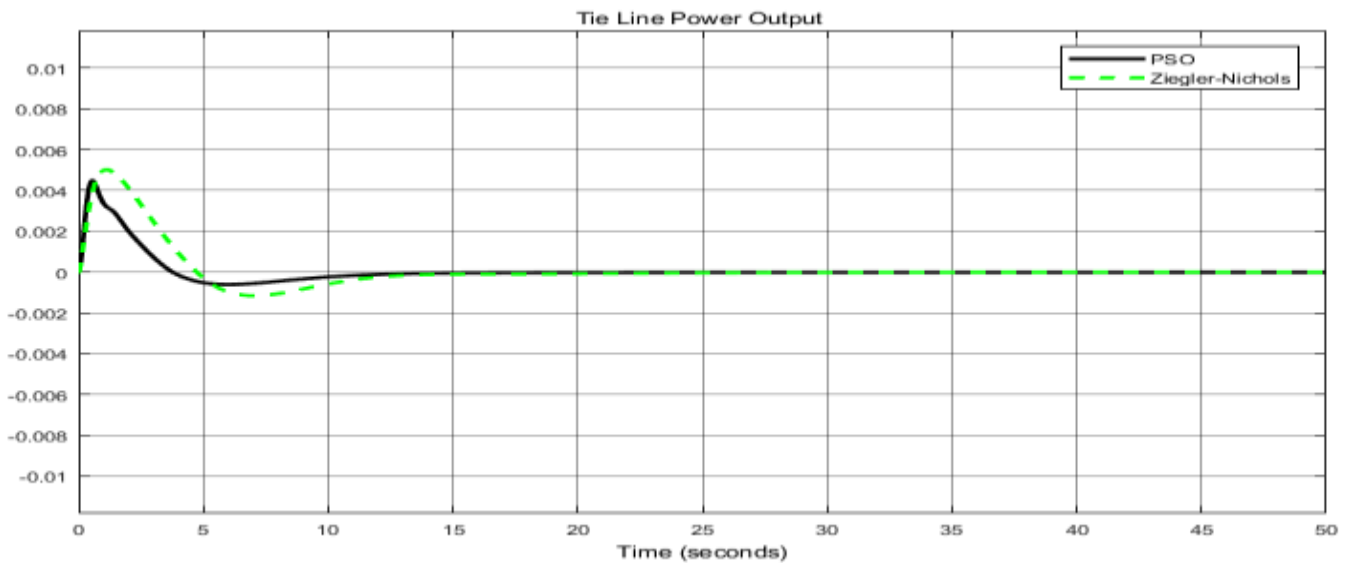


Figure 10: Deviation of the transmission line power to load changes in region 2

The power fluctuation curve due to the demand of the second region is given in Figure 10, which indicates power fluctuates from the first region to the second region, and with the optimal performance of the controllers and the reaction of the area controllers power oscillation ultimately reaches to zero. The magnitude of the integral of the squares of the oscillatory power errors in the transmission line for the proposed method and the classical method of Nichols are 23.34 and 54.14, respectively, which indicate the lower oscillation for the proposed method. The amount of overshoot in the proposed method and the classical method, are 0.004 per unit and 0.005 per unit, respectively.

**C. Frequency control results to simultaneous load variations in regions one and two**

In this section, we intend to study the frequency fluctuations of the system in regions 1 and 2 and the oscillation of the power in tie line for the

$\Delta P_{L2,L1} = 0/01pu$ . According to the graphs in Figure 11, the magnitude of the integral of the squares of frequency error for the proposed method and the classical method of Nichols for area 1 are 113.7 and 203.5, respectively, and for the second region, are 135.6 and 224.6, respectively.

The power fluctuations due to the load changes in regions 1 and 2 are given in Figure 12. The magnitude of the integral of the squares of the oscillatory power errors in tie line for the proposed and the classical Nichols methods are 7.44 and 4.85, respectively, which indicate the lower oscillation of the Nichols controller.

Power oscillations in UPFC due to the sudden changes in power in regions 1 and 2 is given in Figure 13, which indicates in the proposed method settling time is lower and power compensation happens faster.

**D. Frequency control results to simultaneous incremental and detrimental load changes in regions 1 and 2**

According to the graphs in Figure 14, the magnitude of the frequency error squares for the proposed and the classical methods in area 1 are 7.96 and 4.28, and for the area 2 are 5.7 and 7.14 respectively which indicate the efficiency of the proposed algorithm in reducing the oscillation of the second region which has received more power.

Power fluctuations in tie line due to the greater power demand in region 2 is given in Figure 15. The magnitude of the integral of the squares of the oscillatory power errors in the transmission line for the proposed method and the classical Nichols are 101.3 and 234.5, respectively, which proved better performance of the proposed controller.

The UPFC power oscillations due to the sudden changes in area 2 power is given in Figure 16, which indicates settling time is less in the proposed method, and the power compensation is faster in the initial moments of the load increase in the second region, UPFC unit compensation power increases 0.005 per unit to improve the network power quality and then, by appropriate operation of area controllers for power compensation, power fluctuations eventually drops to zero.

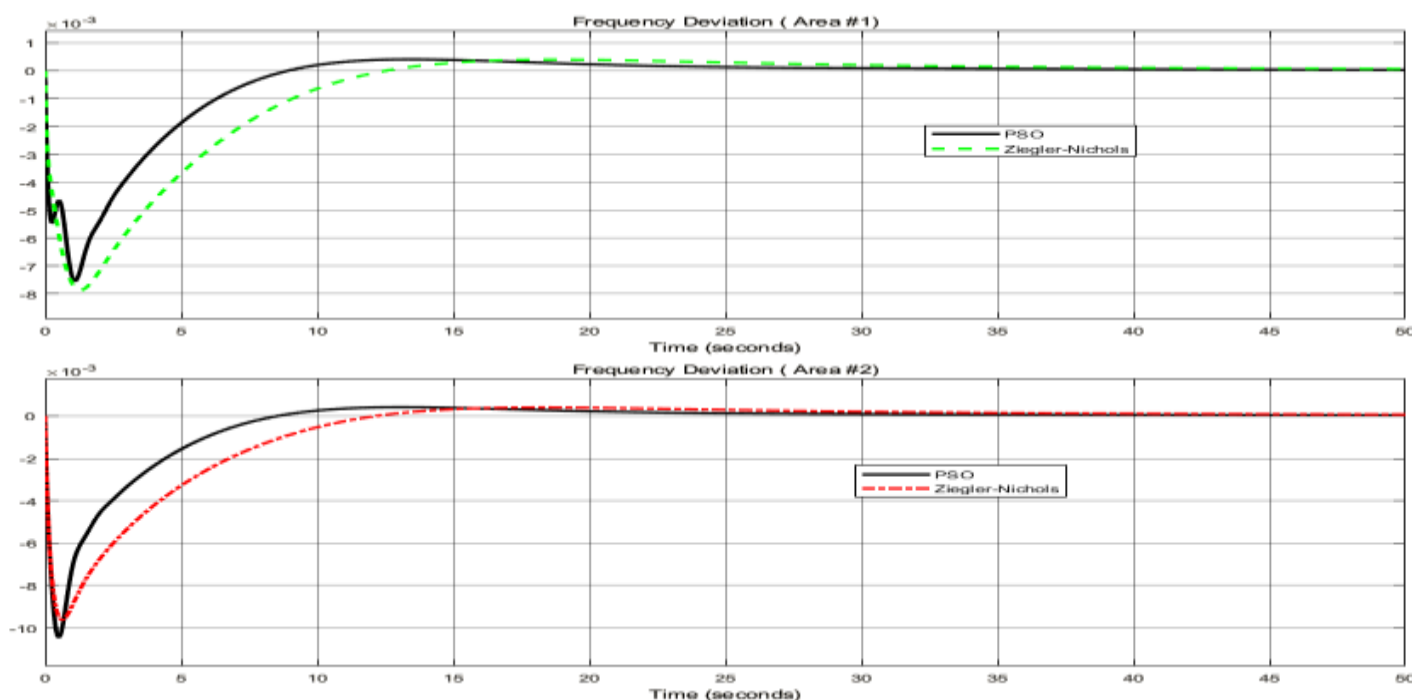


Figure 11 : Frequency deviations in regions 1 and 2 for incremental changes in load

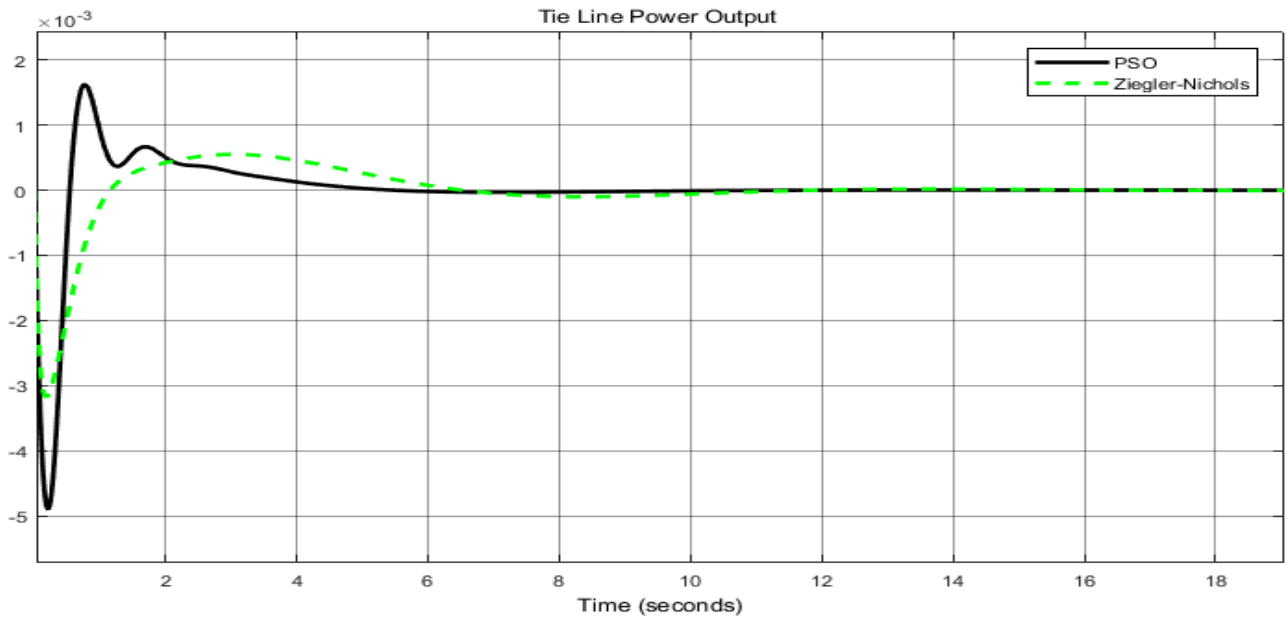


Figure 12: Fluctuations in transmission line power to incremental load changes in areas 1 and 2

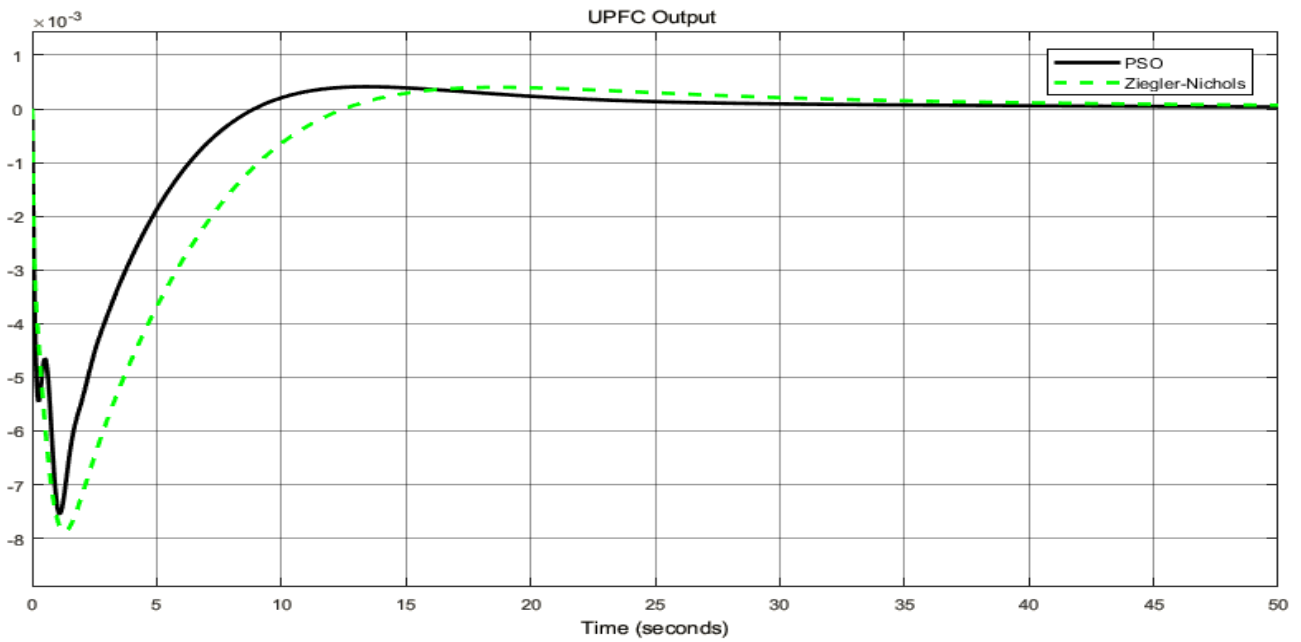


Figure 13: UPFC output power diagram with incremental load changes



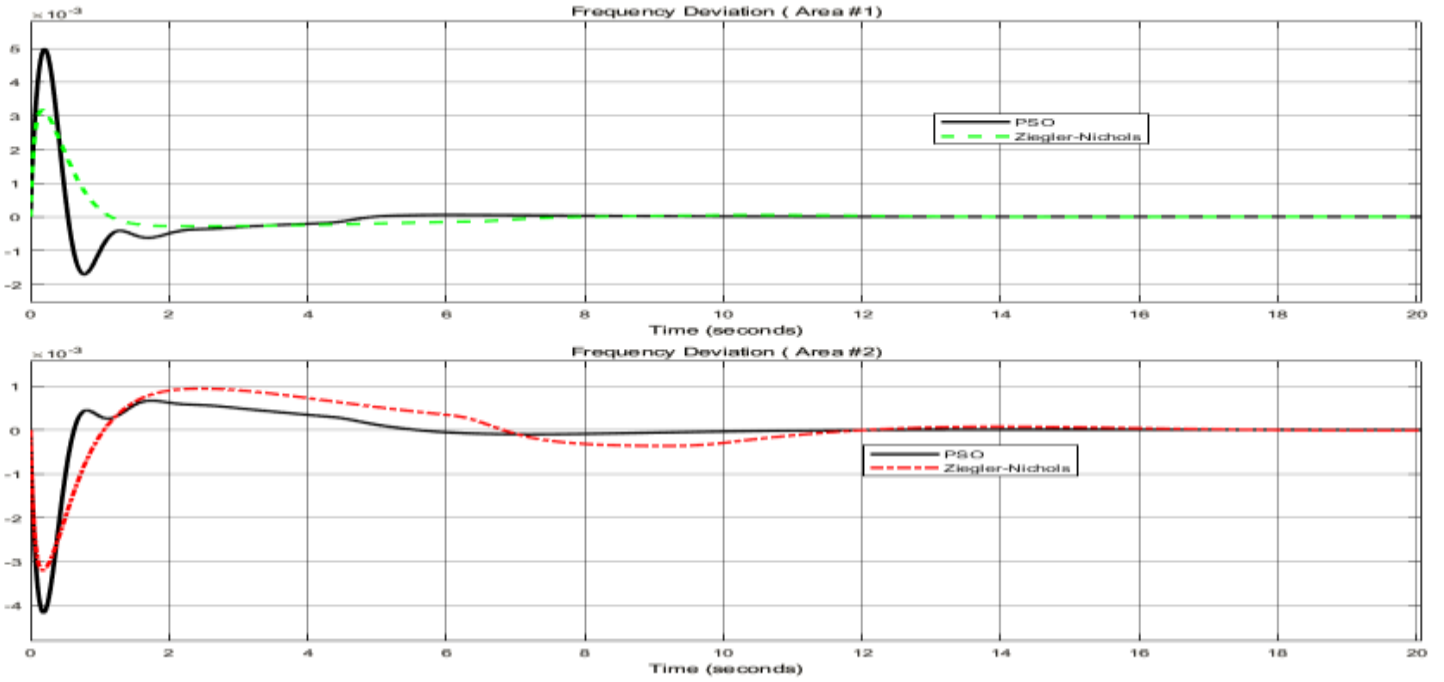


Figure 14: Frequency error with incremental and decremental load changes in regions 1 and 2

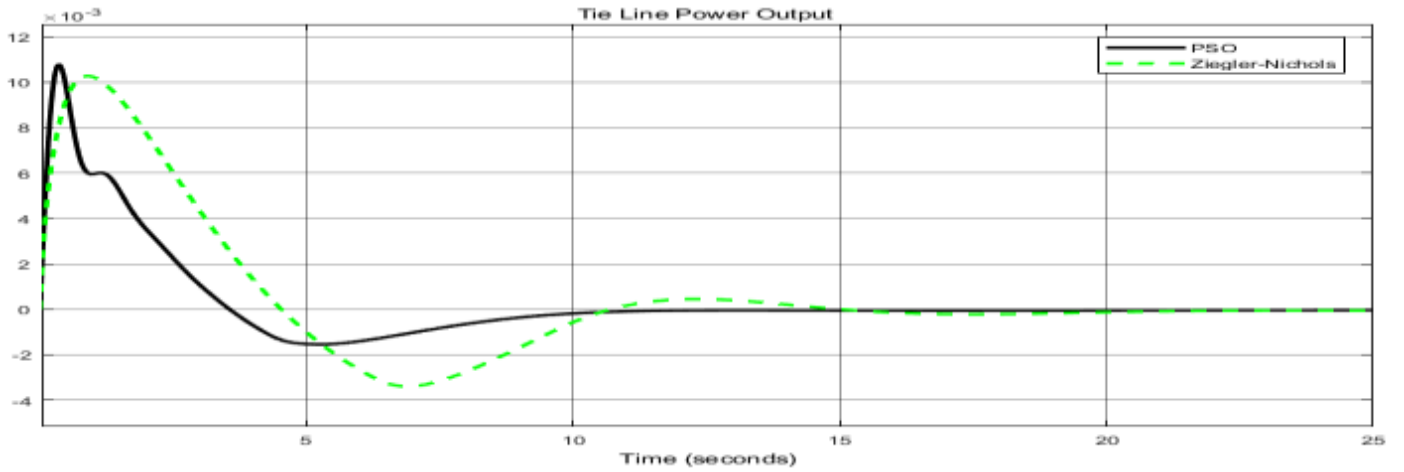


Figure 15: Output power of the transmission line with incremental and decremental load changes

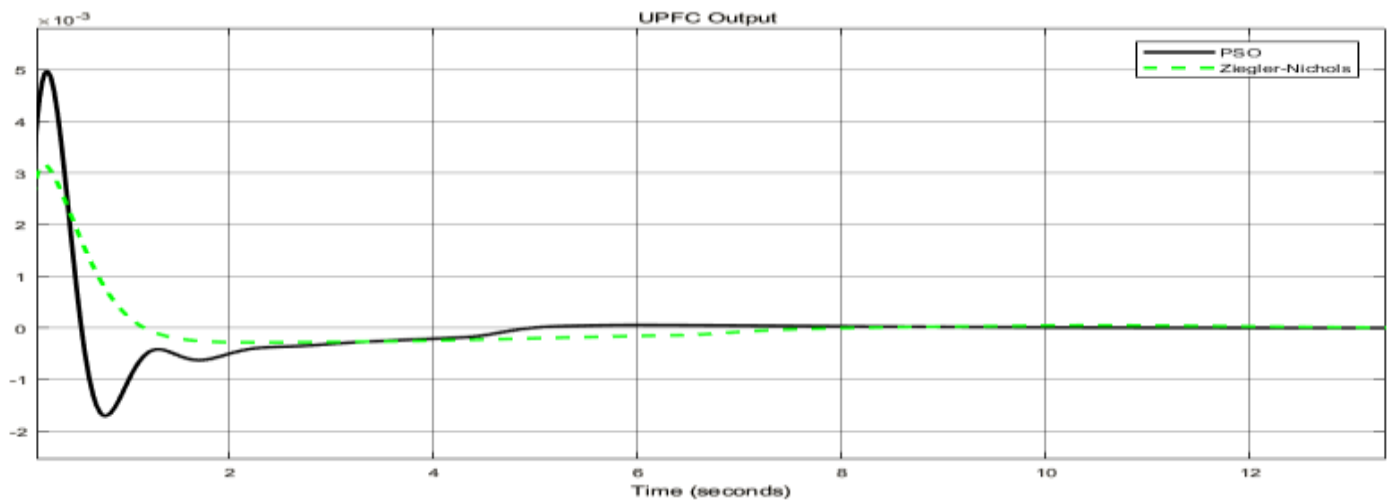


Fig. 16: UPFC output power with incremental and decremental load changes in areas 1 and 2

**E. Frequency control results to random load variations in areas 1 and 2**

In this section, we calculate the frequency oscillations in regions 1 and 2 and the oscillation of the power in the connection line for random variation of  $\Delta P_{L2,L1}$  in the 5% per unit interval and the time variations of the power up to 50 seconds with a simulation time of 500 seconds. Figure 17 shows the variations in the power output of three power units in area 1 for random load changes. From this figure we realize that the steam, water and gas plants operate with a 2% change for balance between supply and demand in area one. In addition, the gas power plant reaction has more overshoot in comparison with the other two power plants, due to the reaction of the fuel chamber to compensate for the fuel.

However, according to Figure (18), the magnitude of the integral of frequency error squares, for the proposed and the classical methods for area 1 are 1563 and 2274 units, and in the second region, they are 1747 and 2473 units, respectively which express a significant decrease in the integral of the frequency error.

The power fluctuations in tie line with random load changes in both regions is shown in Figure 19 and the results for the magnitude of the integral of oscillatory power error squares in the transmission line for the proposed and the classical Nichols methods for exchange power are 1727 and 890, respectively, which indicate a very low oscillation in proposed controller. Since in a real situation, fluctuations and load variations are often unpredictable and random, and transmission power

of the lines plays a crucial role in network stability, then the importance of the role of proposed controller with PSO algorithm is obvious.

The UPFC power compensation diagram for improving the stability of the network and damping of the transmission line fluctuations is illustrated in Figure 20. As we see the settling time and the damping of the oscillations are less in the proposed control mode.

Now we assume that the UPFC is separated from the grid for an unknown cause and there are random-load variations in both regions, then the fluctuations pattern for the transmission line power during UPFC connection and disconnection mode is given in Figure 21, which indicates during UPFC disconnection state and at the time of sudden changes in the load, low frequency oscillations occur between two areas in the power system and eventually due to the dynamics of the power system and the operation of the controllers in each area these oscillations dampen to zero. If UPFC is at the end of the transmission line, due to the rapid response, the series and parallel converters provide the required instantaneous power for the network and the power fluctuations are reduced much faster.

The frequency diagram for the two regions during UPFC connection/ disconnection mode is shown in Figure22. The constructive role of the UPFC in improving the voltage angle at the end of the line and quality of the transmission line power causes the frequency oscillations to be rapidly suppressed when changing the load.

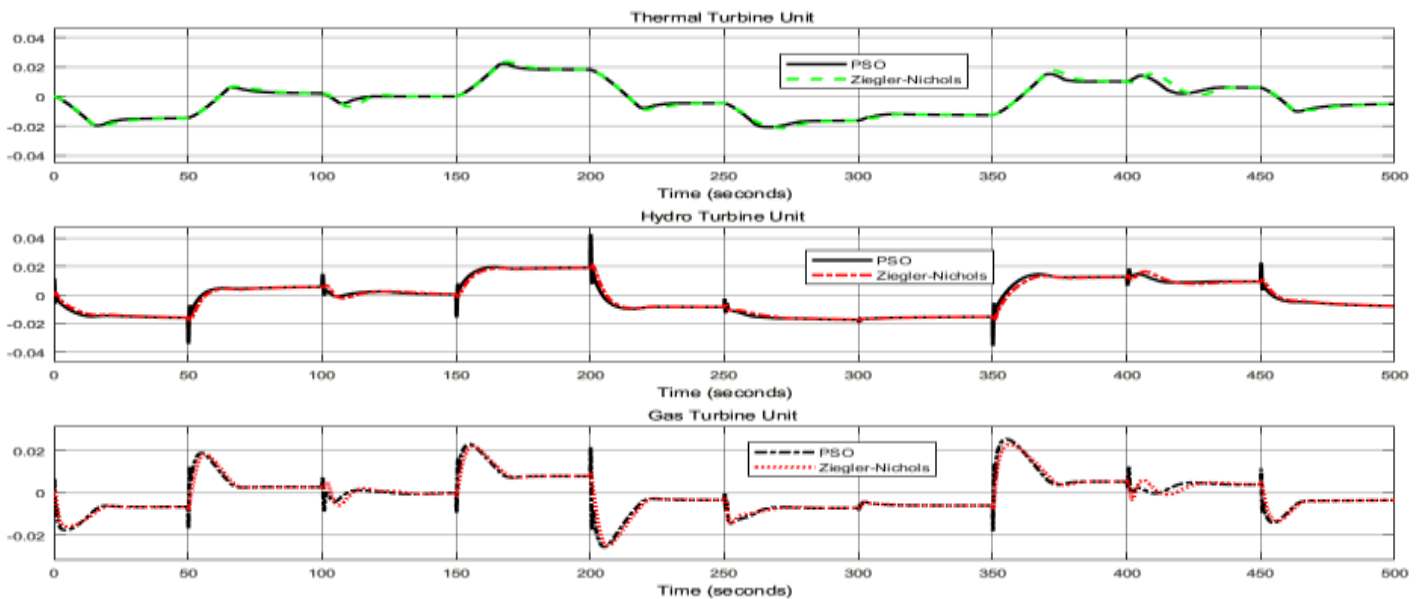


Figure 17 : Turbine output powder diagram in area one with random load variations

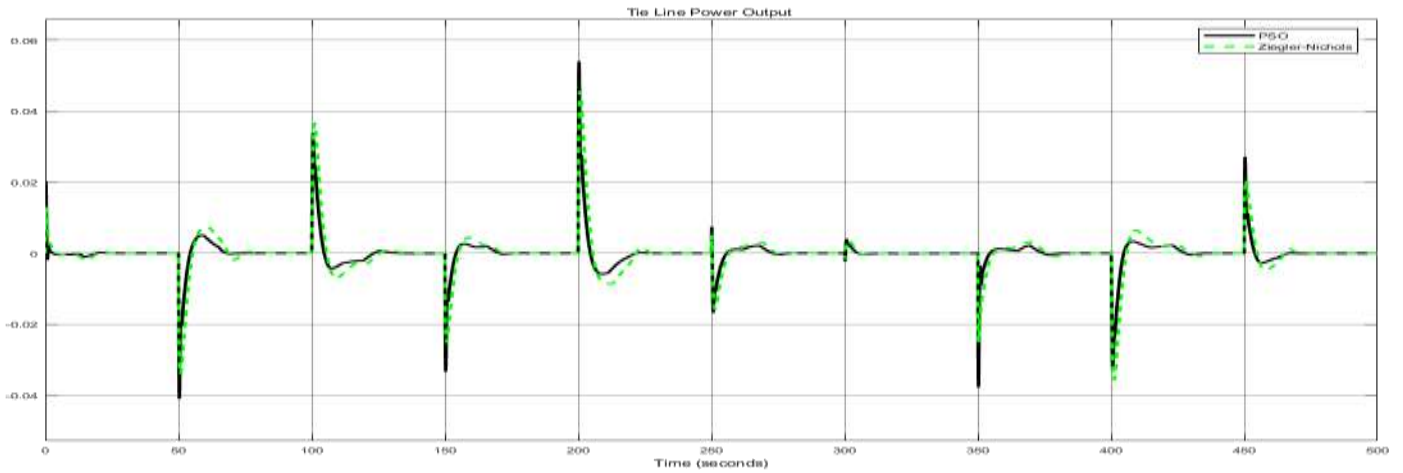


Figure 18: Frequency deviations in areas 1 and 2 with random load variations

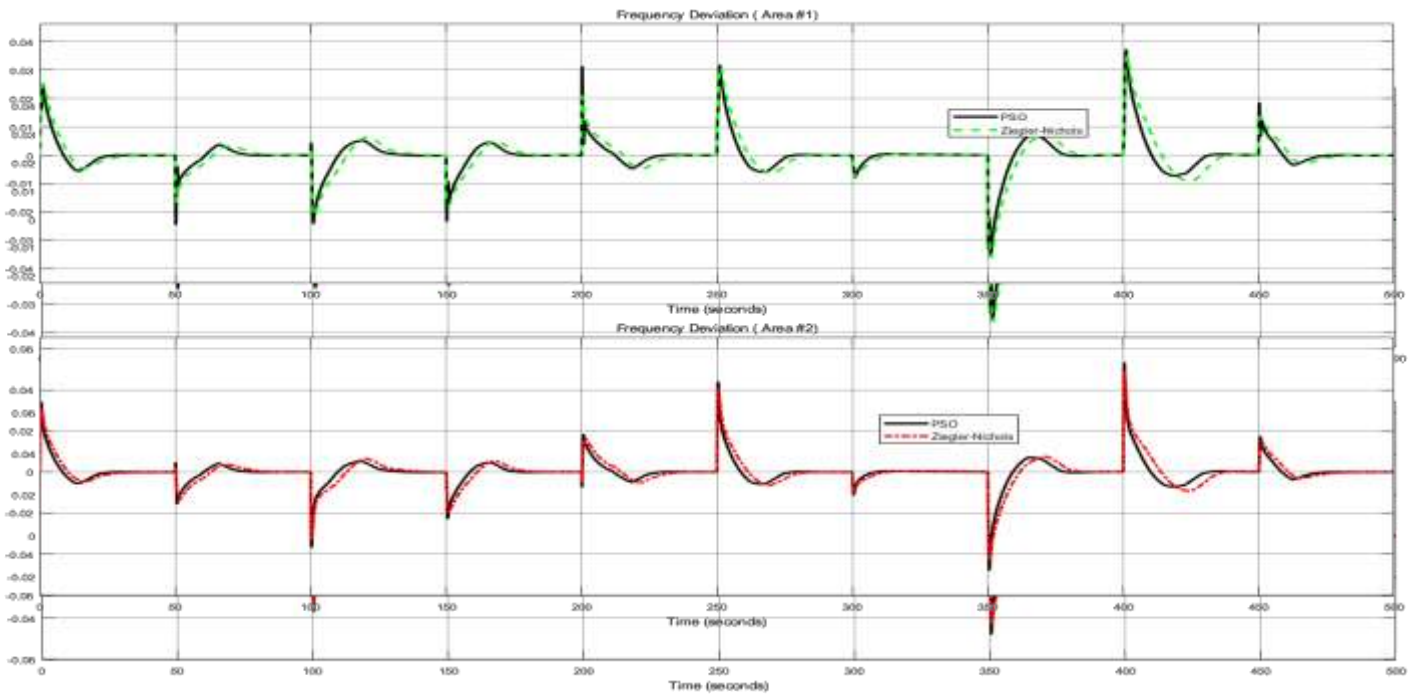


Figure 19: Fluctuations of the output power of the transmission line with incremental load variations

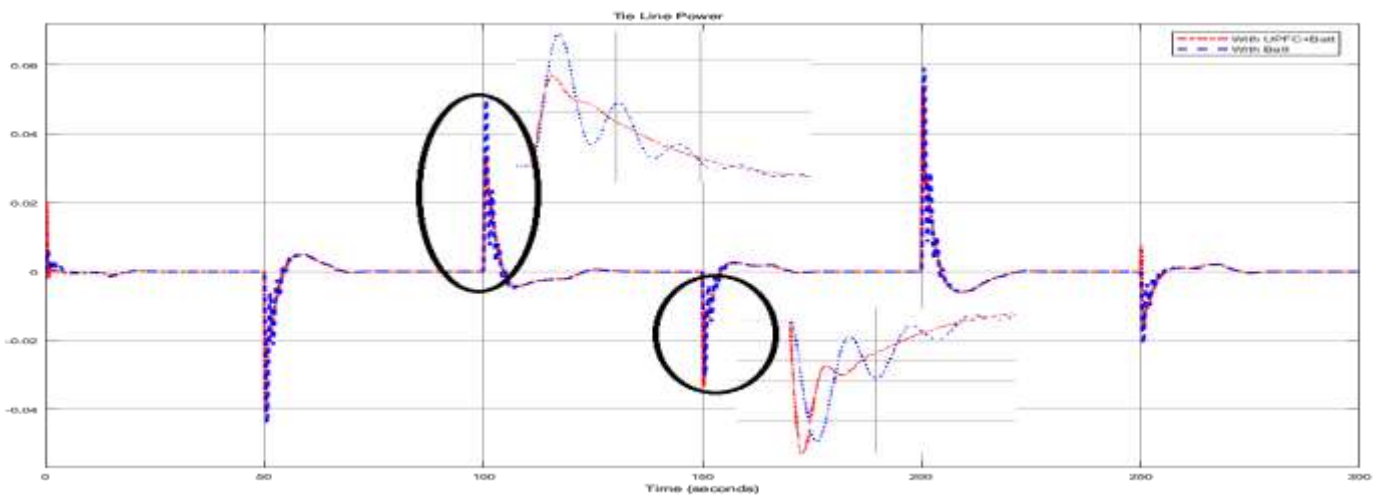


Figure 20: UPFC Output Power with Random load Changes

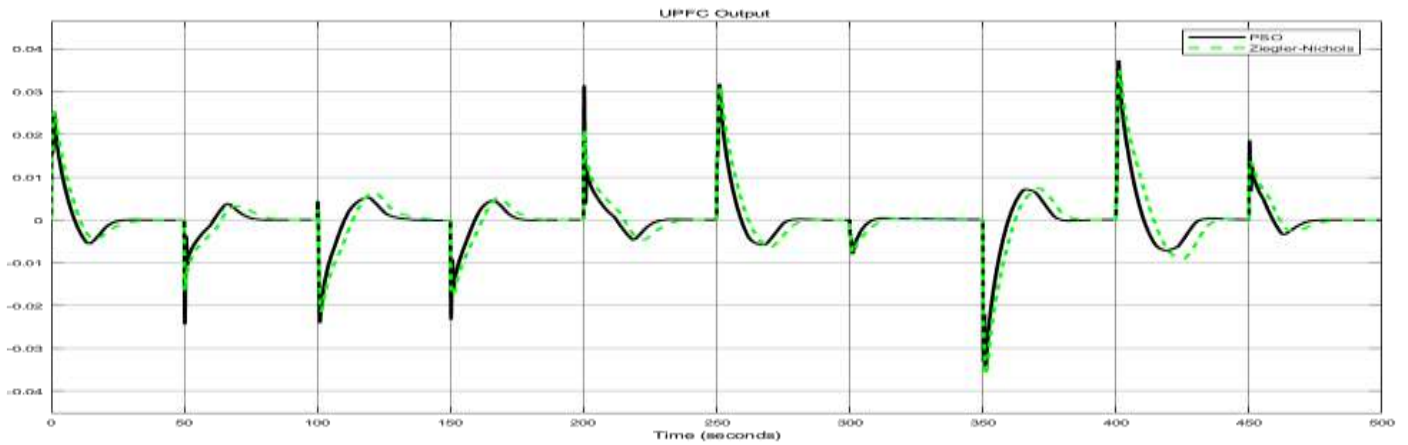


Fig. 21: Transmission line Output Power Oscillations with UPFC connection/disconnection

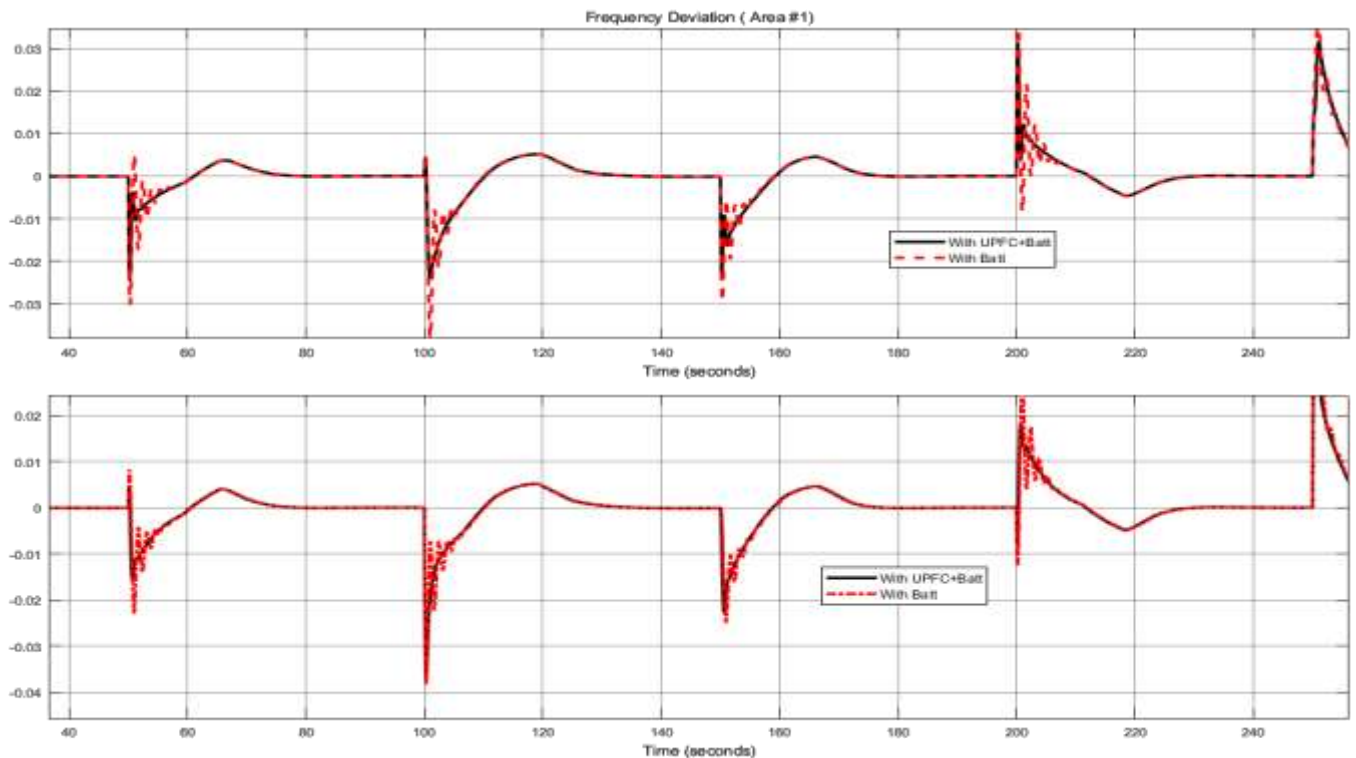


Figure 22: Frequency deviation diagram with UPFC connection/disconnection

**F. Frequency control sensitivity results to changes in parameters of the network operating point**

$T_{12}$  according to equation (2) is the slope of the power angle curve at the point of operation and is called the power synchronization coefficient. Therefore, due to changes in the point of operation of the two-regions with the load distribution, it is necessary that the frequency control system does not disturb and diverge with the change of this coefficient. For this reason, we examine the integral of the frequency error for  $\Delta P_{L1, L2} = 0.01 \mu\text{p}$ .

$$T_{12} = \left. \frac{dp_{12}}{d\delta_{12}} \right|_{\delta_{120}} = \frac{1E_1 11E_2 1}{X_{12}} \cos \Delta\delta_{120}$$

Figure 23 shows the integral of the square of the frequency error in both regions for the proposed

control and Zikler for the coefficient changes from zero to 50% of the initial value. As we observe, frequency error in the proposed control is always less than classical control and demonstrates a better reliability for field testing.

The steam turbine model should relate the mechanical power output to the position of the steam valve. For this reason with regards to the operating point and accessories such as boiler and reheater, the time constant of the turbine mechanical system is a function of the operating point. Therefore, it is necessary that the frequency control system does not suffer from disturbances and divergence issues due to the changes in turbine mechanical time constant.

Figure 24 shows the integral of the square frequency error for both areas in terms of the turbine time

constant changes from zero to 50% of its initial value using a  $\Delta P_{L2,L1} = 0/01pu$ . The frequency error with increasing power synchronization coefficient in the proposed control is always less than the classic

control and in both regions, the frequency error is almost independent of the operating point of the steam system and would be constant.

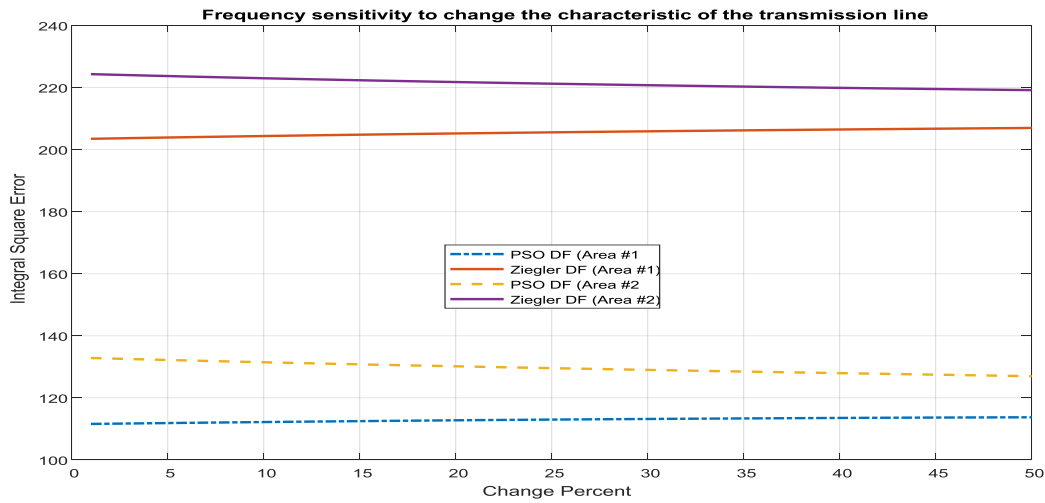


Figure 23: Sensitivity diagram for frequency deviations to the changes of transmission line characteristics

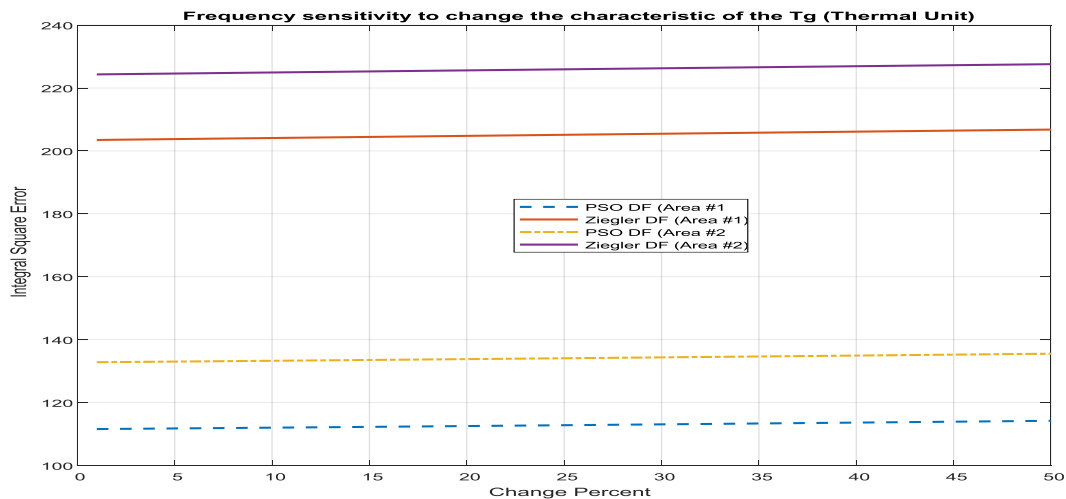


Figure 24: Sensitivity diagram for regional frequency deviations in terms of steam turbine time constant

Figure 25 shows, the same procedure is also valid for the hybrid turbine, and with an increase in the time constant of the hybrid turbine, the frequency fluctuations has a smooth and constant gradient. In each area of the power system, according to equation (3), velocity, regulating coefficient R plays a determining role in controlling the frequency and power fluctuations in the network.

$$R_i = -\frac{\Delta F}{\Delta P_{Gi}} \quad i = 1, \dots, m$$

In this research, the value of this coefficient for all power plants in both regions was considered 2.4 Hz/per unit Megawatt. Since R changes in terms of design, it is necessary to determine the frequency

controller's sensitivity to this coefficient. For  $\Delta p_{L1,L2} = 0.01 pu$ , Figure 26 shows the variations of the integral of the square of the frequency error in both regions for proposed control and Zikler for R variation from zero to 50% of its initial value. The figure indicates an increase in the frequency error in both regions proportional to the increase in speed coefficient R. This increase in frequency error in the proposed PID controller with bird algorithm, is less than classical method. On the other hand, in frequency control systems to apply a complete control, in addition to the frequency variations, the tie line power variations has to be also considered as a

feedback variable. The linear combination of these two quantities is considered as the input to the controller. According to equation (4), the coefficient B is called the Regional frequency bias coefficient or regional frequency response characteristic. It is necessary to examine the effect of the frequency response characteristic of the region on the frequency control function. Integral of the square error to changes in parameters B<sub>1</sub> and B<sub>2</sub> is shown as a decreasing function in Figure 27. The amount of reduction in the proposed controller is less than the

conventional method, and with increasing the bias characteristic of each area, the frequency settling time is lowered.

$$ACE_1 = \Delta P_{12} + B_1 \Delta f_1$$

$$ACE_2 = \Delta P_{12} + B_2 \Delta f_2$$

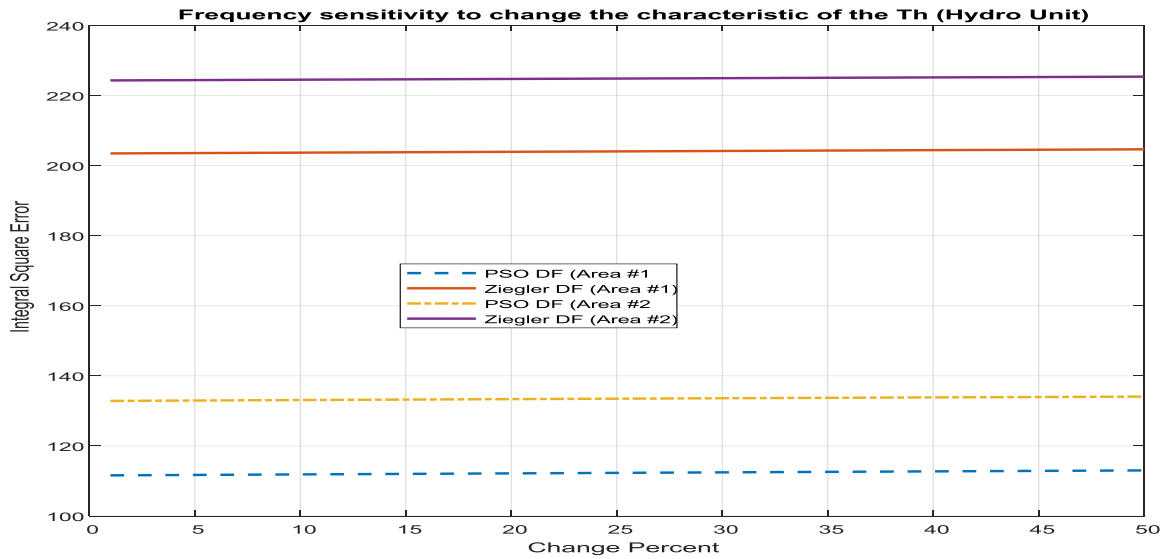


Figure 25: sensitivity diagram for regional frequency deviations in terms of Hydro Turbine time constant

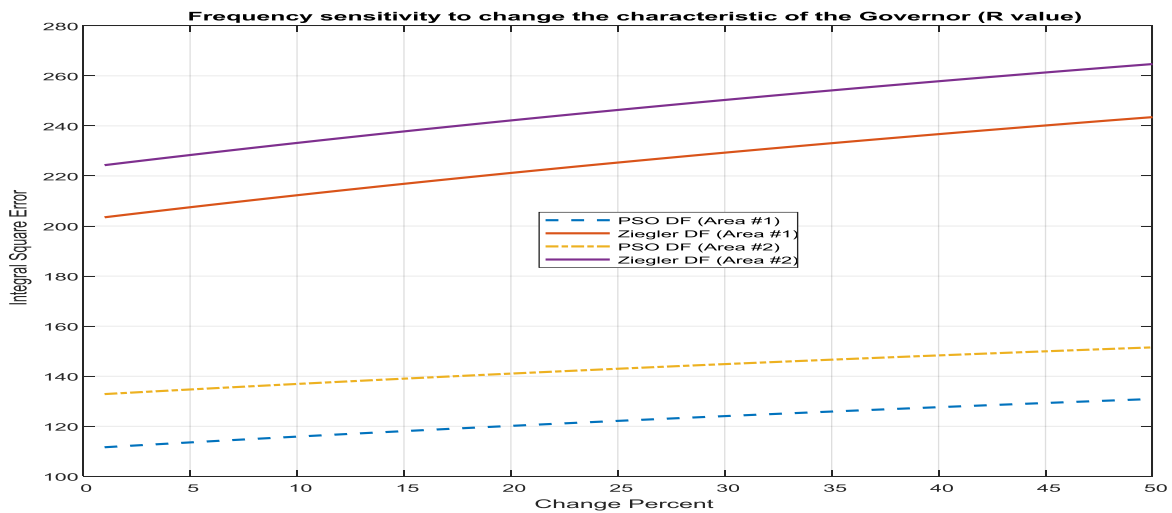


Fig. 26: frequency Sensitivity to changes in characteristic of the governor

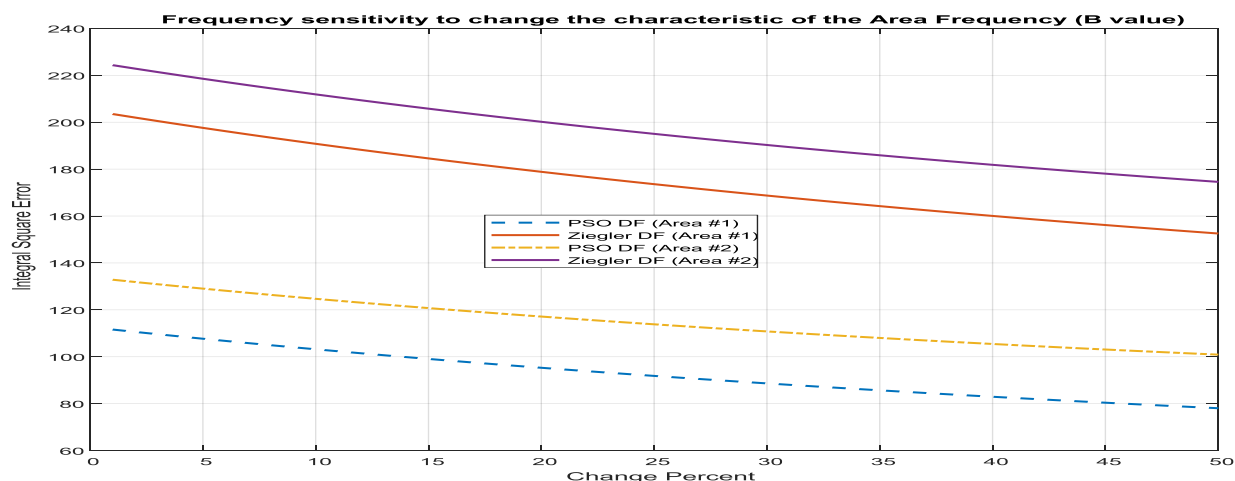


Figure 27: Frequency sensitivity deviations to the frequency characteristic variations of the region

#### IV. Conclusion

The frequency stability of a power system depends on the real power balance, and since the frequency is a common factor throughout the system, any changes in the actual power demand at any point is reflected as a frequency variation across the system. The power required by a large power system is supplied by a large number of generators, so the power demand needs to be divided among the units. Of course, the load distribution between generators and the initial control of speed is made by the governors mounted on the generators, but for the precise regulation of the frequency at the nominal amount, there would be a need for a supplementary control which must be carried out in a main control center. In a continuous power system, frequency control equipment and automatic voltage control are installed on each generator. Controllers are configured to operate under certain conditions and control, voltage, and frequency. For small load changes small variations in actual power depend mainly on the variation in the angle of the rotors and consequently on the frequency. The reactive power is also dependent on the size of the voltage (or, in other words, the generator's stimulation). Frequency control of loads and stimulation control would be investigated separately. The main objectives of frequency control are to keep the frequency at nominal value, to divide the system load between generators in a desirable and economical way, and to adjust the amount of power exchange within the planned values. In fact, the change in system frequency and the actual power should be eliminated by the change in production. Line signals or in other words  $\Delta P$  and  $\Delta F$ , are amplified and combined then converted to the actual command signal  $\Delta P_v$ , which should be sent to the primary drive to make the input power changes as desired. Therefore, the unit's drive will also change its  $\Delta P_v$  output power and causes  $\Delta P$  and  $\Delta F$  to be minimized. One of the most

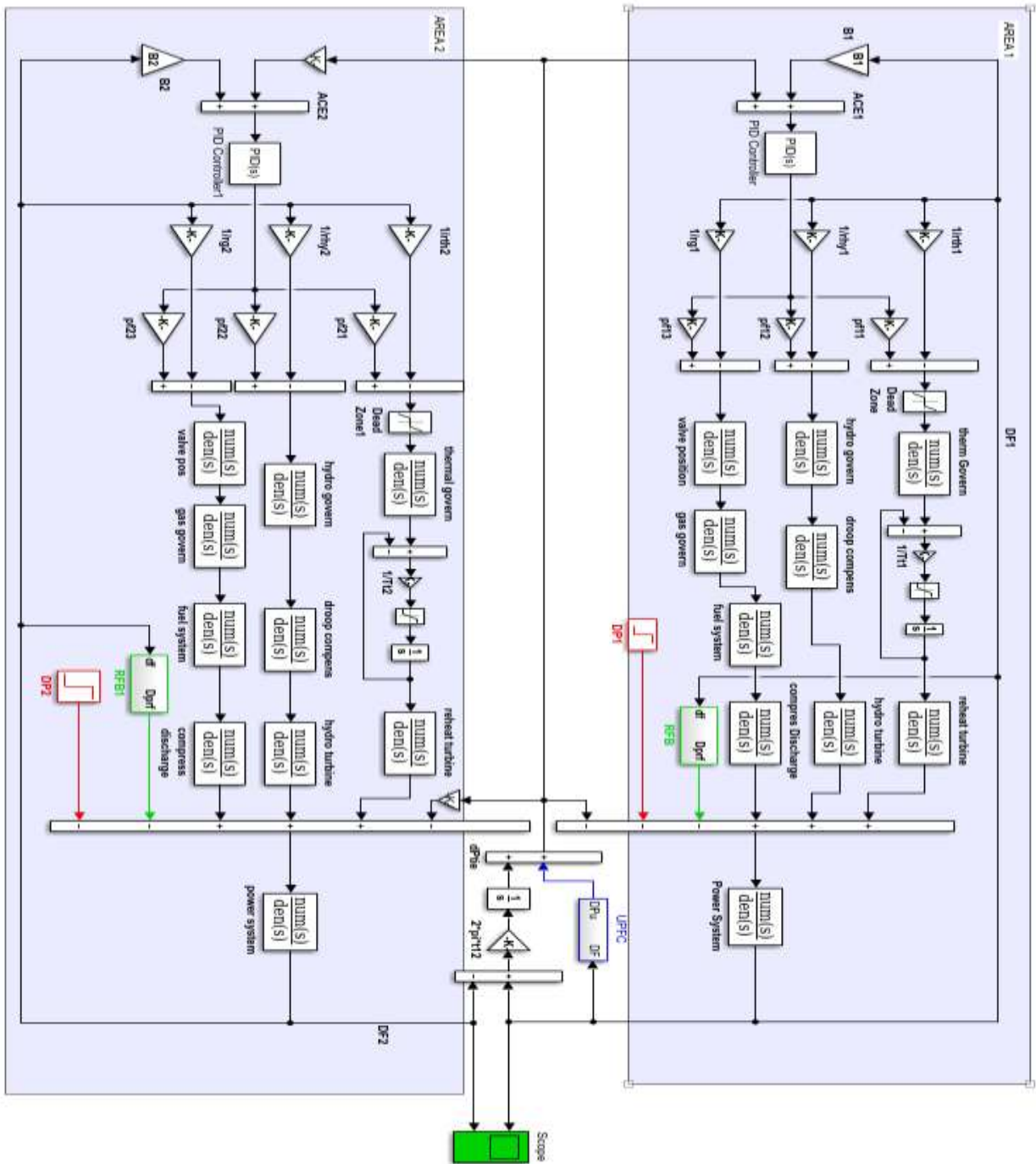
important advantages of using FACTS devices in the transmission system is the increase of the transient stability margin of the power system, which is performed by controlling active and reactive power of the line during an error occurring in the system. Although the power system stabilizer is the most important tool for damping the fluctuations, but in some places it does not have the ability to dampen the fluctuations, so the use of FACTS equipment is a good solution to this problem. In this paper, UPFC has been used to simulate fluctuations and improve transient stability, and PSO algorithm has been used to optimize PID controller parameters. From computer simulation results, the effect of UPFC with conventional PID controller for simulating local and inter-regional fluctuations, under small disturbances in a two-area network has been studied and the efficiency of the proposed algorithm has been demonstrated.

#### References

- [1] Abdelaziz, A. Y., & Ali, E. S. (2016). Load frequency controller design via artificial cuckoo search algorithm. *Electric Power Components and Systems*, 44(1), 90-98.
- [2] Guha, D., Roy, P. K., & Banerjee, S. (2016). Load frequency control of large scale power system using quasi-oppositional grey wolf optimization algorithm. *Engineering Science and Technology, an International Journal*, 19(4), 1693-1713
- [3] Guolian, H., Lina, Q., Xinyan, Z., & Jianhua, Z. (2012, July). Application of PSO-based fuzzy PI controller in multi-area AGC system after deregulation. In *Industrial Electronics and Applications (ICIEA), 2012 7th IEEE Conference on* (pp. 1417-1422). IEEE
- [4] Hingorani, N. G., Gyugyi, L., & El-Hawary, M. (2000). *Understanding FACTS: concepts and technology of flexible AC transmission systems* (Vol. 1). New York: IEEE press
- [5] Pappachen, A., & Fathima, A. P. (2016). Load frequency control in deregulated power system integrated with SMES-TCPS combination using ANFIS controller. *International Journal of Electrical Power & Energy Systems*, 82, 519-534
- [6] Pradhan, P. C., Sahu, R. K., & Panda, S. (2016). Firefly algorithm optimized fuzzy PID controller for AGC of multi-area multi-source power systems with UPFC and SMES. *Engineering Science and Technology, an International Journal*, 19(1), 338-354

- [7] Rakhshani, E., Remon, D., & Rodriguez, P. (2016). Effects of PLL and frequency measurements on LFC problem in multi-area HVDC interconnected systems. International Journal of Electrical Power & Energy Systems, 81, 140-152
- [8] Shankar, R., Chatterjee, K., & Bhushan, R. (2016). Impact of energy storage system on load frequency control for diverse sources of interconnected power system in deregulated power environment. International Journal of Electrical Power & Energy Systems, 79, 11-26
- [9] Shiva, C. K., & Mukherjee, V. (2016). Design and analysis of multi-source multi-area deregulated power system for automatic generation control using quasi-oppositional harmony search algorithm. International Journal of Electrical Power & Energy Systems, 80, 382-395
- [10] Shree, S. B., & Kamaraj, N. (2016). Hybrid Neuro Fuzzy approach for automatic generation control in restructured power system. International Journal of Electrical Power & Energy Systems, 74, 274-285
- [11] OGHABNESHIN, H. (2019). Two-area power system stability analysis by frequency controller with UPFC synchronization and energy storage systems. Master thesis, Islamic Azad University, Alborz, Iran

Appendix



Simulink model of two-area system